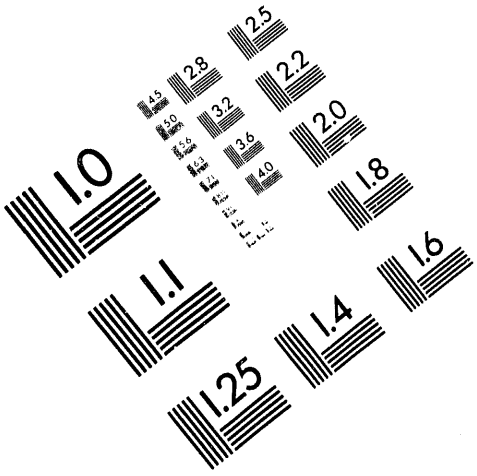

AIIM

Association for Information and Image Management

1100 Wayne Avenue, Suite 1100
Silver Spring, Maryland 20910

301/587-8202

Centimeter

1 2 3 4 5 6 7 8 9 10 11 12 13 14 15 mm

1 2 3 4 5

Inches

MANUFACTURED TO AIIM STANDARDS
BY APPLIED IMAGE, INC.

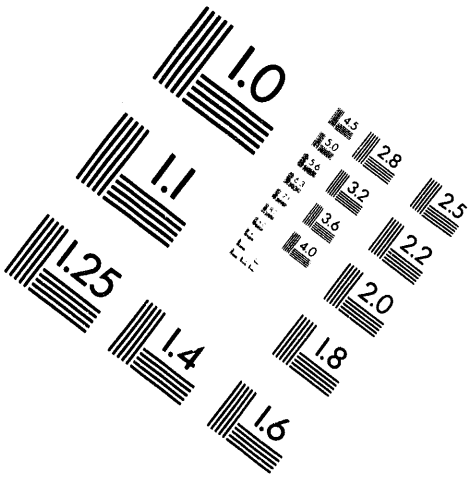

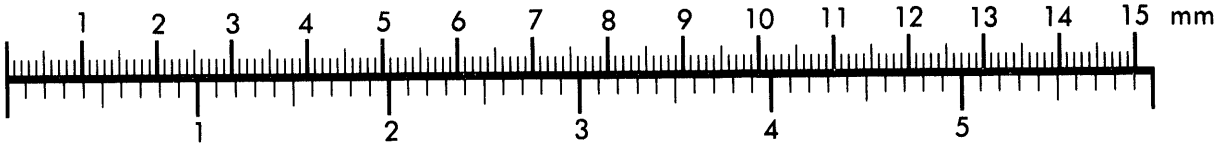

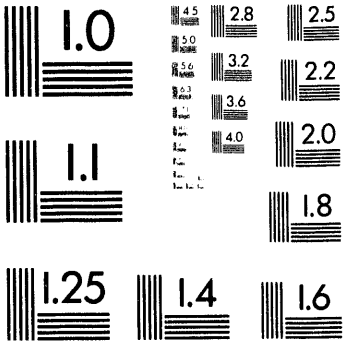

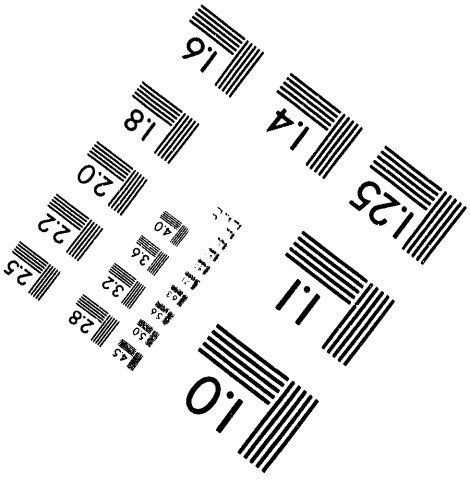

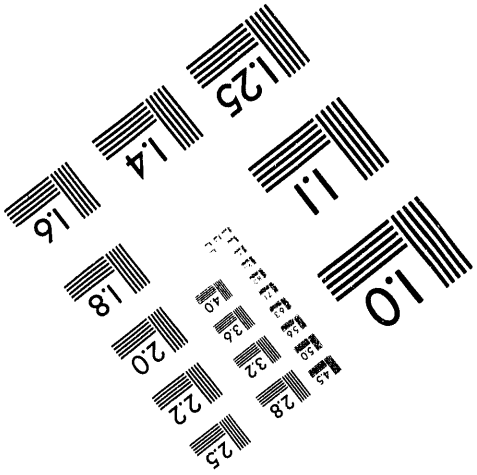

1 of 1

HANFORD CATEGORY C ~~65~~ 44C

[redacted]

BNWL-B-89

1

BATTELLE-NORTHWEST
RECEIVED
MAY 11 1971
REFERENCE COPY
TECHNICAL INFO. SECTION

DECLASSIFIED

CPTF RUN 6 FLUX MONITORING

MAY 7, 1971

[redacted]

[redacted]

ROUTE TO	P. R. NO.	LOCATION	FILES ROUTE DATE
AEC Chem. Officers 63019		Fed	AUG 12 1971
for J. P. Dickinson			

MASTER

[redacted]

DECLASSIFIED

BATTELLE-NORTHWEST
PACIFIC NORTHWEST LABORATORIES DIVISION
BATTELLE MEMORIAL INSTITUTE
P. O. BOX 999, RICHLAND, WASHINGTON 99352

BNWL-B-89

Battelle
Pacific Northwest Laboratories

Project Number

Internal Distribution

TF Demmitt
RL Dillon
WW Roberts
SR Wages-KAPL
BNW Tech. Files
JRD - File/LB

Date October 11, 1971

To Distribution

From J. R. Divine

Subject Amendments to BNWL-B-89, "CPTI Run 6 Flux Monitoring" May 7, 1971 (CONFIDENTIAL)

- In Figure 1, Run 6 IRTS Assembly, the footnote "**" should read

  "Distance to upstream end of the test section, ± 1/16","

  not "...of the specimen holder...."

  The dimensions to the upstream ends of the specimen holders are 119" for TS4D and 218 9/16" for TS4U. These dimensions are shown in Figure 1 but were not specially labeled.

- Figure 2 was inadvertently reduced in size during duplication. For reference it may be noted that the restraining sleeve (E) has an I.D. of 0.4" and an O.D. of 0.5".

- In Tables III, IV, V, VI, VII, and VIII, the footnote "Relative to the upstream end of test section" should read "Relative to upstream end of specimen holder." Specimen holder is defined as items C and D in Figure 2.

- The thermal flux values of 3.9×10^{13} on pages 5, 11, 21, 24, and 25 should be corrected to 3.82×10^{13}.

- In Figure 4, a solid line should be placed after the word calculation in the legend to indicate that the solid curves are based on theory. Further, each solid curve should be displaced 0.9" to the right, based on the scale given for the abscissa.

THIS MEMO IS UNCLASSIFIED

[redacted]

BNWL-B-89

HANFORD CATEGORY C-65

Classified By R R Dillon

Classification Cancelled and Changed To
DECLASSIFIED
By Authority of CG-PR-2,
WA Snyder, 2-9-94
By Jerri Marley, 2-17-94
Verified By J E Sawyer 2-23-94

CPTF RUN 6 FLUX MONITORING

J. R. Divine

Corrosion Research & Engineering Section
Fuels & Materials Department

May 7, 1971

This report is intended primarily for internal use by the sponsoring organization and Battelle-Northwest.

[redacted]

This document contains restricted data as defined in the Atomic Energy Act of 1954. Its transmittal or the disclosure of its contents in any manner to an unauthorized person is prohibited.

Group 1 Excluded from automatic downgrading and declassification.

DECLASSIFIED

[redacted]

DISTRIBUTION:

Offsite:

Knolls Atomic Power Laboratory

1. S. R. Wages

Onsite:

Battelle-Northwest

2. T. F. Demmitt

3. R. L. Dillon

4. J. R. Divine

5. W. W. Roberts

6 and 7. Classified Files

[redacted]

DECLASSIFIED

CPTF RUN 6 FLUX MONITORING

J. R. Divine

INTRODUCTION

At the present stage of reactor coolant studies it is possible to say that radiation affects the deposition behavior of corrosion products in the reactor. A quantitative relation between flux and deposition rate or amount is not available, nor is there information as to exactly which component, or combination thereof, of the radiation is most important.

To determine these effects and those of other process parameters, Battelle-Northwest (BNW) is conducting an experimental program for the Knolls Atomic Power Laboratory (KAPL) to evaluate the behavior of corrosion products in pressurized, water-cooled nuclear reactor systems. This program is authorized by and is being performed under the terms and conditions of KAPL Purchase Order 7730-A (and Amendments).

The primary experimental system used by BNW to perform these experiments is the Corrosion Product Transport Facility (CPTF). This is a high-temperature, high-pressure water, in-reactor loop. It is designed to operate over a wide range of experimental conditions, and to maximize flexibility for experimentation involving formation, transport and deposition of corrosion products. It normally is operated in an isothermal mode. The CPTF is operated by the Irradiation Services Unit, Douglas United Nuclear, Inc., under the technical direction of BNW.

In-reactor test sections of the CPTF were installed in a test facility with a specially tailored neutron flux. They were positioned in the test

[redacted]

facility so that the upstream section, TS4U, was located in a region of essentially flat flux profile and the downstream section, TS4D, was in a region with a flux gradient. In addition to these test sections, which were in approximately the same positions as their predecessors in Run 5, there was a third test section just upstream of the TS4U. This test section was designated the "flux enhancement" test section (FETS) and was designed to provide an enhanced beta flux.

The theoretical calculations performed for the CPTF flux monitoring program include an estimate of neutron energy spectrum for both TS4U and TS4D and an estimate of the beta flux in the FETS. These are described briefly in the discussion.

This report is primarily concerned with transmitting the flux monitoring data for Run 6. Because data from Runs 4, 5 and 6 are now available however, a comparison of these data with one another will be made. Furthermore, though exact cross-sections are not available, some of these data will be converted to the corresponding neutron flux and will be compared to the flux spectrum calculated theoretically. A complete compilation of the neutron spectrum will be deferred until the spectrum is unfolded from the activity data using cross-sections given as functions of neutron energy.

SUMMARY AND CONCLUSIONS

This report transmits the results of the flux monitoring program for CPTF Runs 4, 5 and 6, a summary of the results of the calculated neutron flux spectra for TS4U and TS4D and the beta flux calculations for the flux enhancement test section (FETS) of Run 6. All of the data thus presented are in terms of the operating power level of Run 4, <u>including</u> the beta

flux estimated for the Run 6 FETS. The relative power levels for Runs 4, 5 and 6 were 1, 0.975 and 0.925 respectively; these factors are multipliers for their respective flux data.

Neutron Flux

The thermal neutron flux in the core test section was 3.9×10^{13} n/cm^2sec. For the edge test section it ranged from about 5×10^{12} n/cm^2sec down to 5×10^7 to 5×10^6 n/cm^2sec depending on the particular run (in Run 4, the test section was positioned so that the gradient was about five orders of magnitude, Runs 5 and 6 had about six orders of magnitude variation). All of the experimental data are in good agreement from run to run and, to the extent it has been examined, in good agreement with the calculated flux spectrum. The experimental data have only been partially converted into terms of neutron flux; this conversion will be the subject of the final report on Runs 4, 5 and 6 flux monitoring.

Beta Flux

The beta flux profile in the Run 6 FETS has been calculated. Based on the Run 4 operating power level, the maximum beta flux, directly over the rhodium source, was about 3.6×10^{13} β/cm^2sec (57 nano-amperes/cm^2). This is about 13,000 times greater than over the unenhanced portion of the test specimen.

On the surface of the specimen the beta flux is constant at 3.6×10^{13} β/cm^2sec. The flux decreases an average of 30% in passing from the specimen surface to the top of the water channel, 0.025 inch above the specimen.

EXPERIMENTAL

System

The same basic system was used in Run 6 as in Runs 4 and 5. There were sufficient changes however to make it worthwhile describing it in this report. The location of the IRTS is illustrated in Figure 1. The relationship between the positions shown and KE Reactor may be obtained from BNWL-CC-2620 (SECRET). It will be observed that TS4U is approximately 1/16" nearer the edge of the reactor than in Run 5; the upstream end of the specimen holder is approximately 218 1/16" from the flange reference position. TS4D is approximately 1 5/8" farther from the edge of the reactor than in Run 5; the upstream end of the specimen holder is 119" from the flange reference position.

Test Sections

An in-reactor test section is shown in cross-section in Figure 2. It is based on the same basic design as in Run 5 but uses (a) a narrow flow channel, 0.100 inch by 0.025 inch instead of 0.300 inch by 0.050 inch, and (b) a narrow specimen, 0.200 inch instead of 0.350 inch wide.

The flux monitor channel contained the standard flux monitors described below.

Flux Enhancement Test Section (FETS)

The FETS was used in Run 6 to provide a test section in which the beta flux at the test specimen was significantly different than that in the other IRTS. The FETS differed from the usual IRTS in that it was shorter (it contained one 10-inch specimen rather than three). The cross-section was basically the same as for the other

DECLASSIFIED

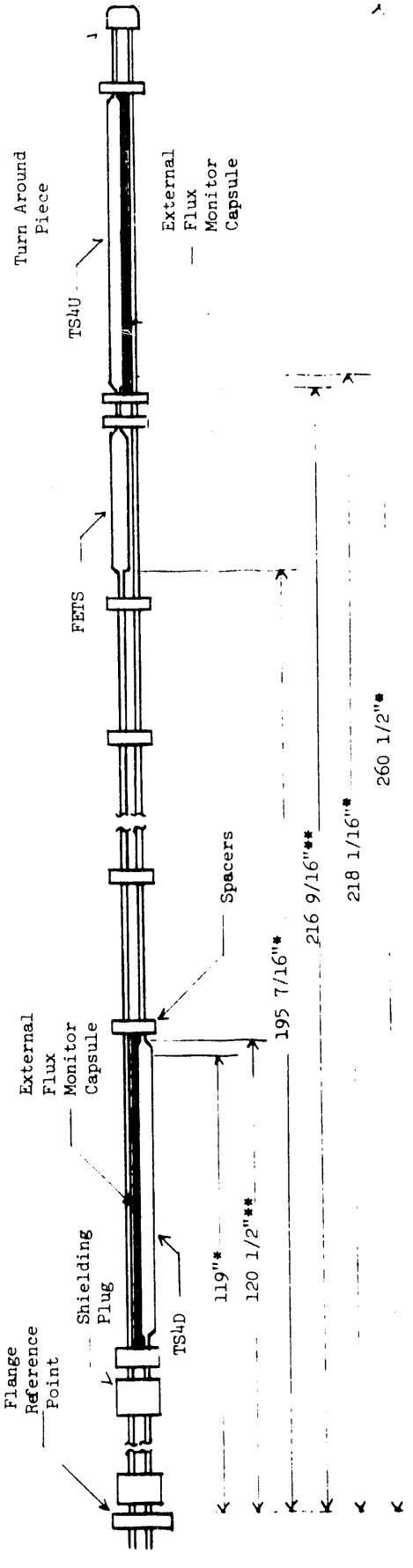

* ± 1/16"

** Distance to upstream end of the specimen holder, ± 1/16".

FIGURE 1 - Run 6 IMTS Assembly.

DECLASSIFIED

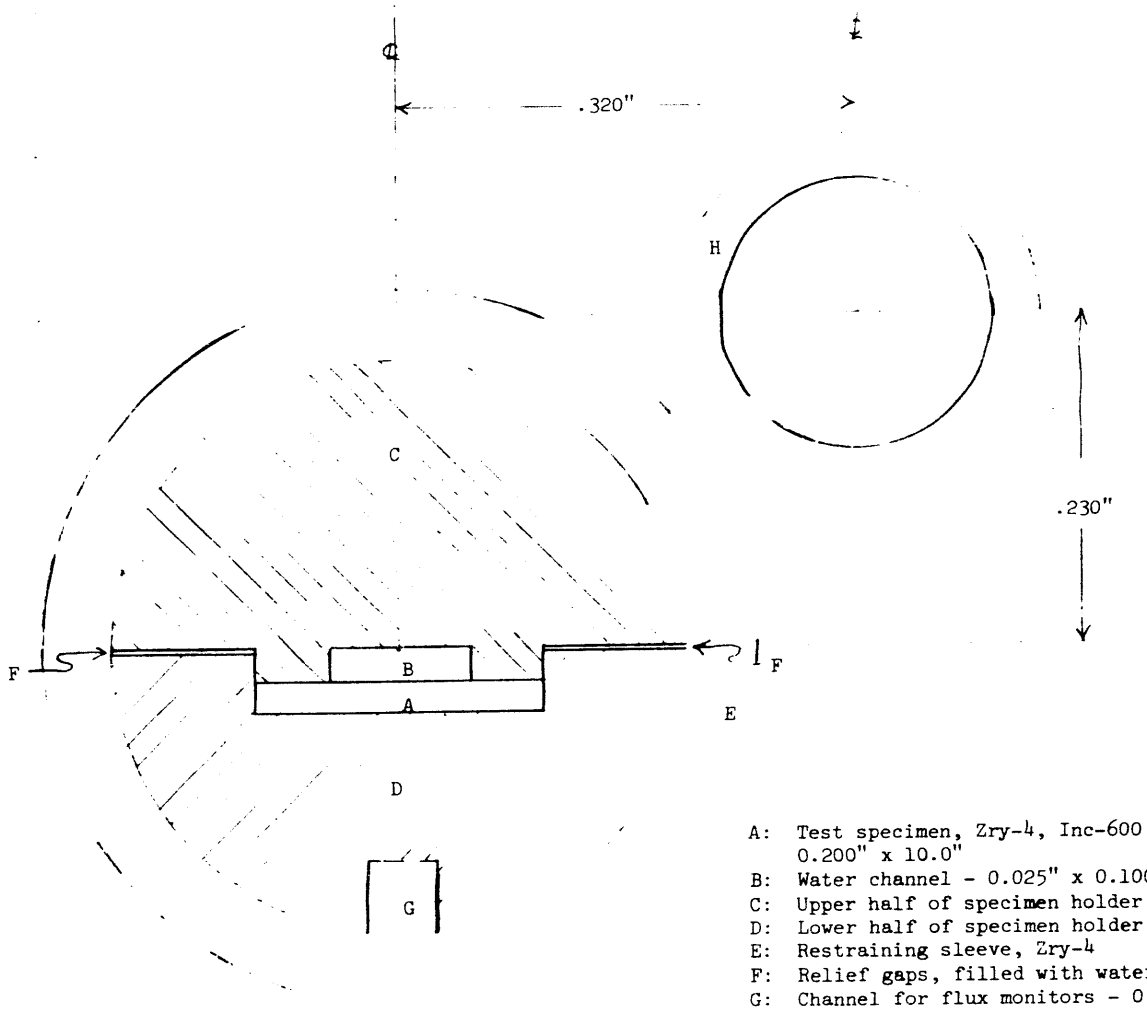

A: Test specimen, Zry-4, Inc-600 or 347 S/S - 0.020" x 0.200" x 10.0"
B: Water channel - 0.025" x 0.100"
C: Upper half of specimen holder
D: Lower half of specimen holder
E: Restraining sleeve, Zry-4
F: Relief gaps, filled with water - 0.005" x 0.100"
G: Channel for flux monitors - 0.050" x 0.052"
H: Spectral Flux monitor capsule

Scale 1" = 0.1"

FIGURE 2 - Cross-Section of the IRTS.

DECLASSIFIED

IRTS: the FETS did not however contain a slot for flux monitors. In addition, under the center four inches of the 10 inch test specimen, a slot, the width of the specimen and 0.010 inch deep, was milled into the specimen holder. A rhodium strip, 4.0 x 0.20 x 0.010 in, was inserted in the slot to act as a beta source.

Rhodium was chosen as a beta source because it has a high thermal neutron capture cross-section (149 barns) and a short half life (4.36 min for Rh-104 m and 42 sec for Rh-104). Further, it occurs naturally as 100% Rh-103. An important requirement was that it is chemically inert (unlike silver which is also a good beta source). Rhodium also provides 2.47 MeV betas which permitted it to be placed below the test specimen and still provide a large beta flux.

In addition to the enhancement of the beta flux, the gamma flux is also enhanced. This is due to the immediate release of the binding energy when a neutron is captured.

Flux Monitors

Run 6 contained two basic types of flux monitors, the so called "standard" monitors as used in previous runs, and a special set of spectral monitors designed to define the neutron energy spectrum.

The standard monitors consisted of wires, composition in Table I, encapsulated in short (1 1/4" to 4 1/4") stainless steel tubes (0.050 inch O.D., 0.033 inch I.D., welded closed at both ends). The CoAl, AgAl, and Cu wires are considered to be bare spectral wires.

DECLASSIFIED

TABLE I

Standard Flux Wire Composition

Wire	Composition (wt %)
Fe	99.99% Fe, 0.003% Si, 0.002% Mg
CoAl	0.1% Co, 99.8% Al, < 0.01% Cu, < 0.01% Ag
AgAl	0.1% Ag, 99.8% Al
Cu	99.999% Cu

The spectral sets were selected and prepared by the BNW Irradiation Effects Section. They were comprised of the materials listed in Table II.

TABLE II

Spectral Flux Monitor Compositions

Wire	Composition (wt %)
Fe	99.99% Fe, 0.003% Si, 0.002% Mg
CoAl	0.1% Co, 99.8% Al, < 0.01% Cu, < 0.01% Ag
AgAl	0.1% Ag, 99.8% Al
Cu	99.999% Cu
AuAl	0.13% Au, 99.87% Al
Ti	99.96% Ti, 0.020% Mn, 0.005% Fe, 0.005% Ni
Pu^{238}	99.48% Pu^{238}, present as PuO_2
Np^{237}	94.52% $N;^{237}$, present as NpO_2
U^{238}	99.989% U^{238}, present as U metal
U^{235}	93% U^{235}, present as U metal

The spectral sets were located approximately 0.4 inches from the standard monitors (at closest approach), more precise figures are in Tables III and IV; their relative positions are shown in Figure 2. These spectral sets were constructed by placing the wires and fission capsules listed in Table II in a 0.18 inch O.D., 0.10 inch I.D., 1 1/4 inch long gadolinum cylinder which was fitted with end caps. Each of these Gd capsules constituted a set of spectral monitors. Four each of these sets were encapsulated in Zry-4 tubing. The spectral sets were positioned in the Zircaloy tubing so that they were immediately adjacent to the bare spectral wires in the standard sets (i.e., adjacent to the capsules containing CoAl, Cu, and AgAl wires).

RESULTS AND DISCUSSION

All activities from Runs 4, 5 and 6 have been reduced to saturation activities per parent nucleus (dps per atom) for reactor power level equal to that in Run 4. Run 5 was actually at a 2.5% lower power than Run 4; therefore, the flux values should be lowered 2.5%. Similarly, Run 6 operated at a level 7.5% below Run 4. These data have been collated in Tables III through XI. From the form presented, the data may be converted to flux (n/cm^2sec) by dividing each number by the respective neutron cross-sections. For example, in TS4U the Fe-58 (n, γ) Fe-59 activity, Tables III to V, averages 4.55×10^{-11} dps/atom. The thermal neutron cross-section is 1.2 barns. Based on this number, the thermal neutron flux is 3.8×10^{13} n/cm^2sec ± 4%. Similarly, from the Co-59 (n, γ) Co-60 data (σ = 37 barns) a flux of 4.0×10^{13} n/cm^2sec ± 2% is obtained. The average thermal flux used is 3.8×10^{13} n/cm^2sec ± 6% (based on Run 4 power).

An estimate of the cross-section for the Fe-54 (n, p) Mn-54 reaction [redacted]

[redacted]

DECLASSIFIED

TABLE III

Run 4 TS4U Saturation Activities

Position*	Position**	Fe-59	Mn-54	Co-60	Ag-110m	Sc-46	Sc-47
0.96	1.15	4.35-11	3.77-13				
5.8	6.0	4.46-11	3.19-13				
9.9	10.1	4.52-11	3.42-13				
10.2	10.35			1.49-9			
10.4	10.6					4.75-14	7.18-14
10.7	10.9				4.96-13		
10.9	11.1	4.49-11	2.88-13				
10.9	11.1	4.61-11	3.39-13				
12.6	12.8	4.46-11	2.83-13				
14.3	14.5	4.49-11	2.83-13				
16.5	16.7	4.35-11	4.11-13				
20.0	20.2	4.52-11	3.53-13				
20.1	20.3	4.55-11	2.88-13				
20.2	20.4			1.49-9			
20.5	20.7					4.67-14	7.72-14
20.8	21.0				4.96-13		
21.1	21.25	4.46-11	3.30-13				
21.3,23.1	21.5, 23.3	4.38-11	3.11-13				
32.6	32.8	4.35-11	3.68-13				
32.7	32.9	4.40-11	3.54-13				
32.8	33.0			1.45-9			
33.1	33.3					4.58-14	6.36-14
33.4	33.6				4.88-13		
33.7	33.9	4.35-11	3.80-13				

* Relative to a reference position in the reactor.

** Relative to the upstream end of the test section.

[redacted]

TABLE IV

Run 5 TS4U Saturation Activities

Position*	Position**	Fe-59	Mn-54	Co-60	Ag-110m	Co-60***
34.6	34.1	4.81-11	3.31-13			
34.3	33.8	4.64-11	3.43-13			
34.0	33.5			1.57-9		
33.7	33.2					2.06-15
33.5	33.0				5.22-13	
33.2	32.7	4.52-11	3.68-13			
31.9	31.4	4.55-11	3.63-13			
30.2	29.7	5.02-11	3.56-13			
29.9	29.4	4.64-11	3.33-13			
29.6	29.1			1.61-9		
29.3	28.8					1.97-15
29.1	28.6				5.33-13	
28.9	28.4	4.73-11	3.13-13			
26.3	25.8	4.52-11	3.33-13			
25.7	25.2	4.55-11	3.06-13			
22.2	21.7	4.55-11	3.17-13			
19.7	19.2	4.38-11	3.23-13			
18.6	18.1	4.52-11	3.33-13			
18.4	17.9			1.53-9		
18.1	17.6					2.13-15
17.8	17.3				4.99-13	
17.6	17.1	4.46-11	3.33-13			
14.7	14.2	4.67-11	3.31-13			
14.5	14.0			1.57-9		
14.2	13.7					1.97-15
14.0	13.5				5.18-13	
13.7	13.2	4.67-11	2.99-13			
11.2	10.7	4.99-11	3.53-13			
9.9	9.4	4.64-11	3.02-13			
7.3	6.8	4.70-11	2.99-13			
6.6	6.1	4.46-11	3.26-13			
3.5	3.0	4.40-11	3.20-13			
3.2	2.7			1.49-9		
3.0	2.5					
2.7	2.2				4.77-13	2.98-15
2.5	2.0	4.35-11	3.23-13			

* Relative to a reference position in the reactor.

** Relative to the upstream end of the test section.

*** From the Cu-63 (n, α) Co-60 reaction

[redacted]

DECLASSIFIED

TABLE V

Run 6 TS4U Saturation Activities#

Position*	Position**	Fe-59	Mn-54	Co-60	Ag-110m	Co-60***
34.7	34.3	4.11-11	2.86-13			
34.4	34.0			1.36-9		
34.2	33.8					2.06-15
34.0	33.6				4.69-13	
33.7	33.3	4.14-11	3.57-13			
31.9	31.5	4.70-11	3.63-13			
29.3	28.9	4.99-11	3.67-13			
28.9	28.5	4.64-11	3.23-13			
28.2	27.8	4.84-11	3.48-13			
26.9	26.5	4.93-11	3.39-13			
24.1	23.7	4.46-11	3.20-13			
23.8	23.4				4.97-13	
23.6	23.2					2.00-15
23.3	22.9			1.46-9		
23.1	22.7	4.46-11	3.13-13			
21.1	20.7	4.61-11	3.47-13			
20.1	19.7	4.46-11	3.76-13			
19.9	19.5			1.47-9		
19.6	19.2					2.04-15
19.4	19.0				4.99-13	
19.1	18.7	4.46-11	2.40-13			
17.6	17.2	4.55-11	3.54-13			
15.6	15.2	4.96-11	2.16-13			
15.0	14.6	4.73-11	2.33-13			
11.3	10.9	4.61-11	3.45-13			
8.5	8.1	4.40-11	5.10-13			
8.3	7.9			1.44-9		
8.0	7.6					1.74-15
7.8	7.4				4.92-13	
7.6	7.2	4.46-11	3.00-13			
5.7	5.3	4.55-11	3.39-13			
2.9	2.5	4.46-11	3.28-13			
2.5	2.1	4.58-11	3.20-13			
2.3	1.9			1.46-9		
2.0	1.6					1.91-15
1.8	1.4				5.29-13	
1.6	1.2	4.46-11	3.19-13			

* Relative to a reference position in the reactor.

** Relative to the upstream end of the test section.

*** From the Cu-63 (n, α) Co-60 reaction.

\# dps/parent nucleus.

[redacted]

TABLE VI

Run 4 TS4D Saturation Activities#

Position*	Position**	Fe-59	Mn-54	Co-60	Ag-110m	Sc-46	Sc-47
-11.7	0.4	6.04-12	4.96-15				
-11.5	0.6			2.00-10			
-11.2	0.9					3.72-16	3.57-16
-10.9	1.2				2.61-14		
-10.7	1.4	6.42-12	4.33-15				
- 9.5	2.6	5.19-12	4.59-15				
- 5.9	6.25	3.73-12	1.36-15				
- 1.3	10.8	1.25-12	1.12-15				
- 1.1	11.0			3.76-11			
- 1.0	11.1	2.17-12	3.03-16				
- .8	11.3					7.35-17	
- .5	11.55				4.06-15		
- .3	11.8	1.02-12					
+ .8	12.85	1.53-12	6.88-16				
2.4	14.5	1.08-12	6.04-16				
4.7	16.8	5.31-13	3.51-16				
8.1	20.2	2.48-14	6.25-18				
8.3	20.4			5.82-13			
8.5	20.6	7.58-14					
8.6	20.7					6.43-18	
8.9	21.0				1.03-16		
9.2 ± .05	21.3 ± .05	1.50-14	1.82-17				
9.2 ± .05	21.3 ± .05	1.63-14	8.49-17				
9.3	21.4	1.97-14	1.94-17				
11.1	23.15	1.07-14	9.27-18				
15.0	27.1	1.39-14	1.63-17				
20.7	32.8	8.28-16					
20.7 ± .05	32.8 ± .05	3.38-16	7.68-19				
20.7 ± .05	32.8 ± .05	3.00-16	3.60-19				
20.9	33.0			8.62-15			
21.2	33.3					2.51-19	
21.5	33.6				1.67-18		
21.7	33.8	1.65-16	3.11-19				

* Relative to a reference position in the reactor.

** Relative to the upstream end of the test section.

\# dps/parent nucleus.

[redacted]

DECLASSIFIED

TABLE VII

Run 5 TS4D Saturation Activities

Position*	Position**	Fe-59	Mn-54	Co-60	Ag-110m	Co-60***
-5.9	0.3	2.95-12	1.06-14			
-5.5	0.7	3.15-12	8.24-16			
-5.3	0.9			9.79-11		
-5.0	1.2					5.17-18
-4.8	1.4				1.11-14	
-4.5	1.7	2.77-12	7.15-16			
-1.9	4.3	1.79-12	5.17-16			
- .7	5.5	1.40-12	4.16-16			
-.3, -.1	5.9, 6.1	1.20-12				
1.3	7.5	9.48-13	1.34-16			
1.6	7.8			2.78-11		
1.9	8.1					1.60-18
2.1	8.3				3.04-15	
2.4	8.6	7.56-13	1.94-17			
3.0	9.2	6.18-13				
6.2	12.4	2.44-13	1.18-16			
7.5	13.7	1.24-13	7.28-17			
8.8	15.0	5.34-14				
9.1	15.3	4.55-14	3.96-17			
9.4	15.6			1.29-12		
9.7	15.9					4.79-19
10.0	16.2				1.28-16	
10.2	16.4	2.42-14	3.17-17			
11.5	17.7	1.48-14				
12.2	18.4	1.08-14				
12.8	19.0	8.69-15	1.01-17			
13.4	19.6	7.76-15				
15.3	21.5	7.26-15	2.53-18			
16.7	22.9	5.95-15				
17.1	23.3	3.85-15	6.33-18			
17.3	23.5			1.06-13		
17.6	23.8					< 2.46-19
17.8	24.0				1.03-17	
18.1	24.3	1.85-15	1.69-18			
20.7	26.9	3.73-16	2.11-18			
20.9	27.1	1.90-16	1.24-18			
24.1	30.3	5.31-17	4.22-19			
24.2	30.6			1.35-15		
24.6	30.8					< 2.46-19
24.9	31.1				4.62-19	
25.2	31.4	2.79-17	4.22-19			

* Relative to a reference position in the reactor.

** Relative to the upstream end of the test section.

*** From the Cu-63 (n, α) Co-60 reaction.

[redacted]

TABLE VIII

Run 6 TS4D Saturation Activities#

Position*	Position**	Fe-59	Mn-54	Co-60	Ag-110m	Co-60***
-6.7	1.1	3.18-12				
-6.5	1.3				1.85-14	
-6.2	1.6					5.67-18
-6.0	1.8			9.89-11		
-5.7	2.1	3.06-12				
-4.8	3.0	2.92-12				
-4.6	3.2	2.74-12				
-4.4	3.4				1.47-14	
-4.2	3.6					4.20-18
-3.9	3.9			7.79-11		
-3.7	4.1	2.35-12				
- .95	6.8	1.46-12				
2.3	10.1	8.93-13				
2.9	10.7	6.94-13				
3.6	11.4	6.18-13				
6.1	13.9	2.82-13				
7.4	15.2	1.80-13				
11.3	19.1	1.68-14				
14.4	22.2	8.17-15				
14.6	22.4			8.42-13		
14.9	22.7					< 1.66-18
15.2	23.0				< 1.24-16	
15.4	23.2	9.98-15				
18.9	26.7	2.17-15				
21.5	29.3	1.50-15				
24.3****	32.1	3.53-16				
24.7	32.5	4.73-16				
25.0	32.8	2.20-16				
25.7	33.5				< 1.24-16	
26.0	33.8					< 1.66-18
26.2	34.0			< 1.41-13		
26.5	34.3	5.01-15				

* Relative to a reference position in the reactor.

** Relative to the upstream end of the test section.

*** From the Cu-63 (n, α) Co-60 reaction.

**** Data below this position do not agree with previous data, see text.

\# dps/parent nucleus.

[redacted]

DECLASSIFIED

TABLE IX

Positions of the Gadolinium Capsules

TS4U

Position*	Specimen
Core	
8.1	SC-4
19.7	SC-3
23.5	SC-2
33.9	SC-1
Edge	
-7.5	SE-4
4.2	SE-3
15.3	SE-2
25.7	SE-1

* Relative to a reference position in the reactor, measured to the center of the Gd capsule.

[redacted]

DECLASSIFIED

TABLE X

Run 6 Spectral Data, Core Saturation Activities#

	SC-1	SC-2	SC-3	SC-4
Fe-59	2.75-12	2.77-12	2.79-12	2.71-12
Mn-54	3.40-13	3.33-13	3.33-13	3.16-13
Co-60	1.81-10	1.77-10	1.78-10	1.70-10
Au-198	3.53-9	3.56-9	3.40-9	3.14-9
Cu-64	1.12-11	0.933-11	0.859-11	0.692-11
Sc-46	4.34-14	4.19-14	4.21-14	3.98-14
Sc-47	8.87-14	8.33-14	9.19-14	8.00-14
Sc-48	1.25-15	1.24-15	1.28-15	1.10-15
U^{235} Ba 140 corrected for 93% U^{235} and fy = 0.061	1.49-9	1.35-9	1.29-9	1.27-9
U^{238} Ba 140 corrected for 99.989% 238 and fy = 0.06	2.01-12	1.98-12	2.04-12	1.80-12
Pu^{238} Ba 140 corrected for 99.48% Pu^{238} not for fy	9.60-14	4.54-13	3.12-12	2.86-12
Np^{237} Ba 140 corrected for fy - 0.058 and 99.52% Np^{237}	1.19-11	1.32-11	1.23-11	1.19-11

dps/parent nucleus.

SE and SC fission foils not corrected for transmutations or for errors due to contributions by impurities.

[redacted]

DECLASSIFIED

TABLE XI

Run 6 Spectral Data, Edge Saturation Activities#

	SE-1	SE-2	SE-3	SE-4
Fe-59	-	9.60-17	1.72-15	1.39-14
Mn-54	-	4.91-18	8.47-17	7.58-16
Co-60	< 7.5-16	8.52-15	7.98-14	6.96-13
Au-198	3.53-15	1.74-13	1.45-12	1.44-11
Cu-64	< 1.5-17	4.70-16	5.30-15	4.72-14
U^{235} not corrected for fy	6.05-17	4.68-15	8.97-14	6.28-13
U^{238} not corrected for fy	< 6.1-19	8.77-18	∿ 3.07-16	1.02-15
Pu^{238} not corrected for fy	< 9.8-16	< 9.1-16	3.21-15	2.32-14
Np^{237} not corrected for fy	< 1.4-16	< 1.3-16	8.69-16	3.92-15

dps/parent nucleus.

SE and SC fission foils not corrected for transmutations or for errors due to contributions by impurities.

[redacted]

for KE Reactor has been estimated at 0.128 barns. From Tables III to V, an average saturation activity of Mn-54 is 3.29×10^{-13} dps/atom. Thus the fast flux, >1. MeV, is about 2.57×10^{12} n/cm^{2}sec. Because the cross-sections of the other reactions are more energy dependent, no attempt is made at this time to determine the effective epithermal flux. This operation will be performed when the entire spectrum is unfolded from the activity data presented in this report.

All three sets of experimental data, after being corrected for variations of the reactor power level, are in excellent agreement with one another except for several of the low activity points from Run 6 TS4D. The Run 6 data were obtained using different instruments than in Runs 4 and 5 which were slightly less sensitive, resulting in some inaccuracy at the low activity levels.

In order to obtain a first approximation to the neutron spectrum, prior to the unfolding of the experimental data, a theoretical calculation was performed. A two-dimensional computer code, 2 DB, was used for this. The calculation was performed down the test section, Z - direction, and outward from the centerline, R - direction. The angular symmetry was achieved by mathematically smearing each component out on the surface of a cylinder whose radius was equal to the distance from the centerline to that component.

As a result of this calculation a spectrum divided into 26 energy groups was obtained. For presentation in this report, these data have been condensed farther into three energy groups: thermal, $\leq$ 0.683 eV; epithermal, >0.683 eV, $\leq$ 1 MeV; fast, > 1 MeV. These data have been normalized to a maximum thermal flux, < 0.683 eV, of 3.9×10^{13} n/cm^{2}sec. The normalized data are plotted in Figures 3 and 4.

In Figure 3, page 22, the solid curves (calculated data) need to be displaced 6.6 inches to the right. For example, the point presently at 8 inches should be at 14.6 inches. The experimental data are correct as shown.

DECLASSIFIED

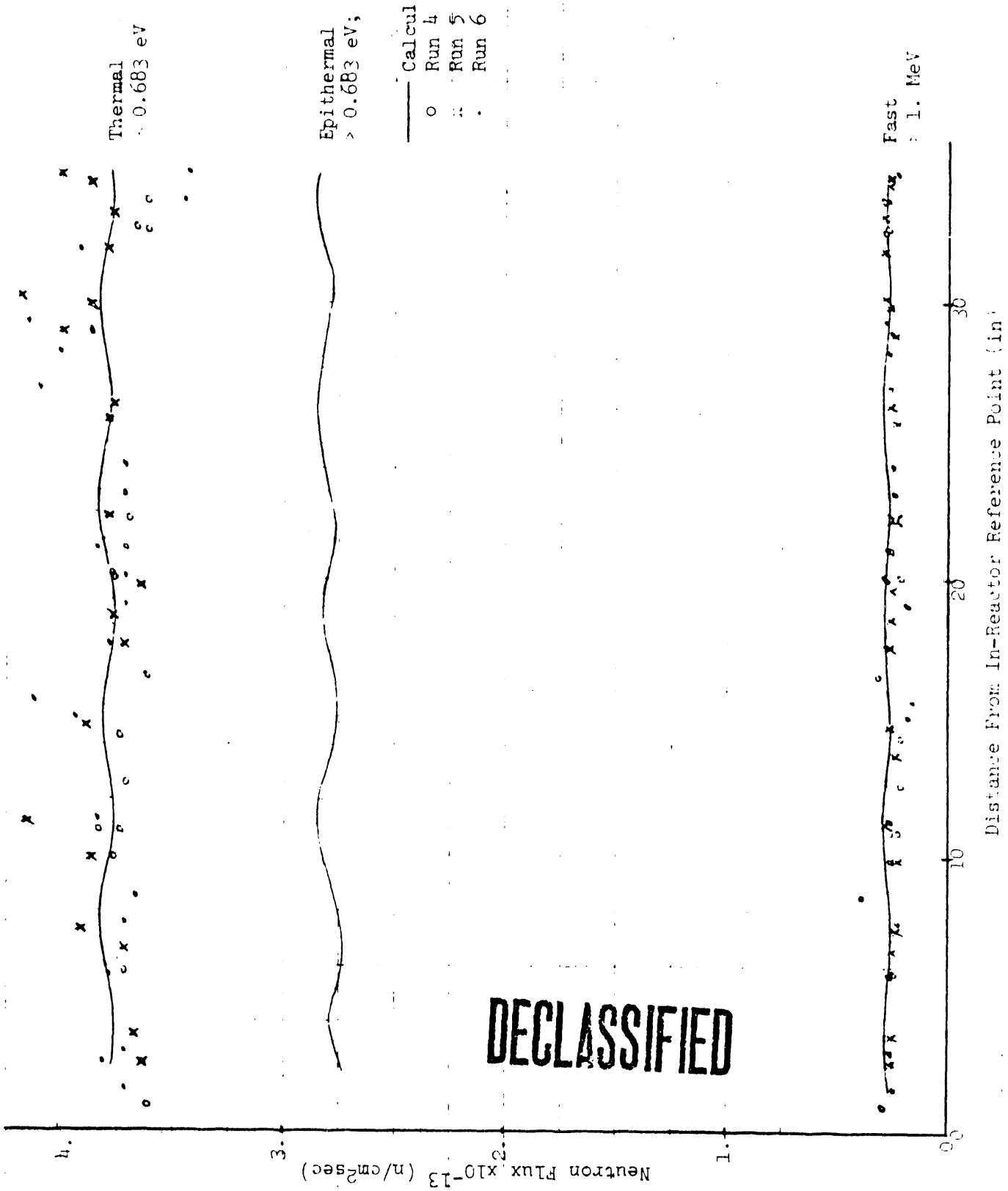

DECLASSIFIED

FIGURE 3 - Neutron Flux in TS4U.

DECLASSIFIED

[redacted]

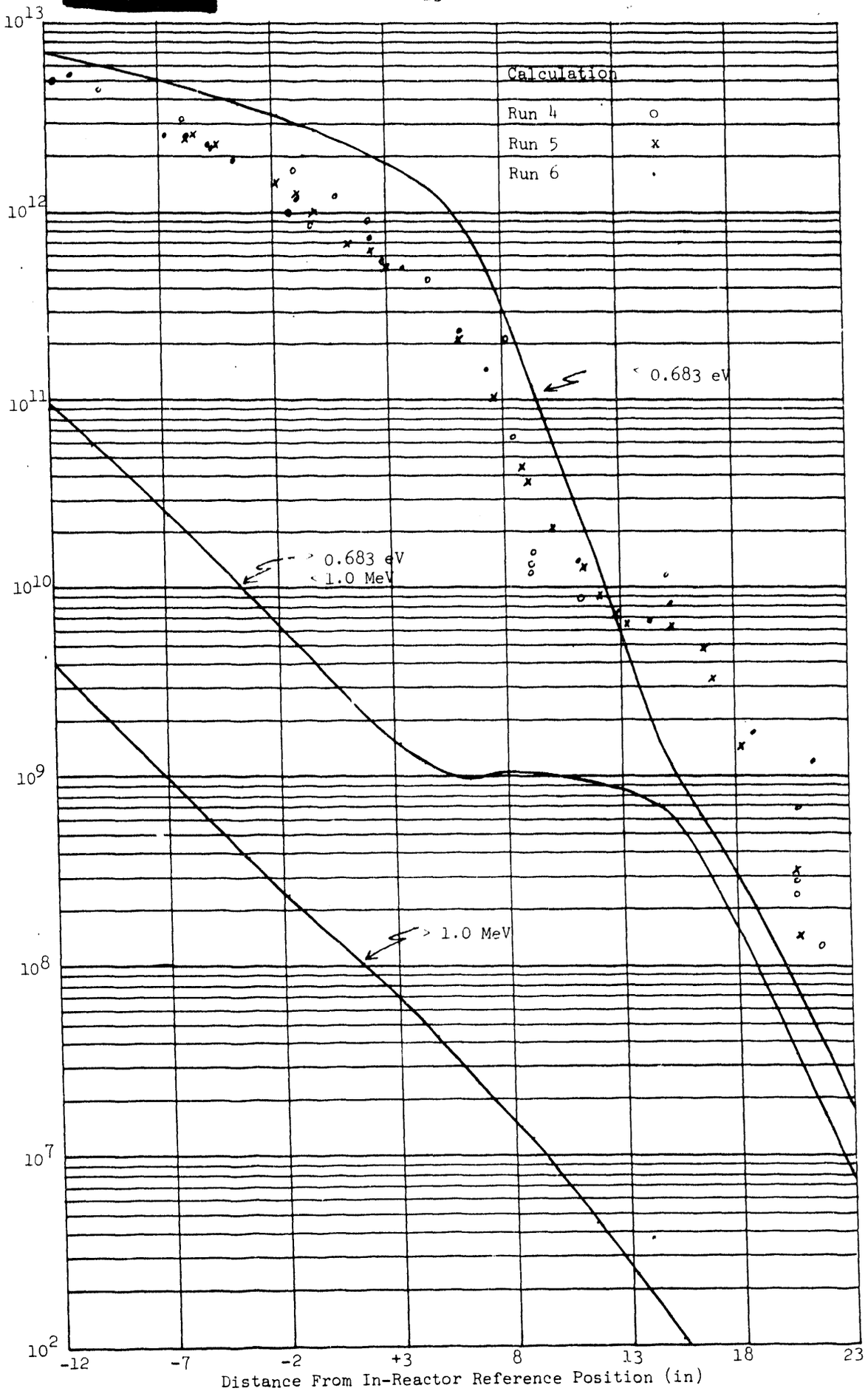

FIGURE 4 - Neutron Flux Profile For TS4D.

[redacted]

In Figure 3, the experimental data for Fe-59 and Mn-54 activities in TS4U have been plotted together with the calculated flux. The calculated thermal flux has been normalized to the average of the experimental thermal data - hence there is no direct comparison. As an indication of the accuracy of the calculation however, it is noted that the calculated fast flux is nearly identical to that obtained experimentally. Further comparisons will be possible when the complete spectrum is obtained.

In addition, it may be observed that the calculated flux has a ripple associated with it due to the spacing of the fuel channels. For the thermal flux, the ripple is about 1%; for the fast flux about 3%. The scatter in the experimental data is greater than these limits; therefore, no ripple is observed except possibly at the 15 and 30 inch positions.

The peaks are more clearly visible in the Run 6 data than those of Runs 4 and 5. Rather being due to a variation in fuel loading it is due to a difference in analytical procedure. In Runs 4 and 5, the activity of the flux monitors was measured for one, approximately ten minute period. In Run 6, each flux monitor was analyzed for four, five minute periods. This provided more statistical information about each monitor than was obtained previously and therefore tended to delineate the peaks.

In Figure 4 the calculated fluxes for TS4D have been plotted, normalized to a core thermal value of 3.9×10^{13} n/cm^{2}sec. Also in this figure is the experimental thermal flux based on the Fe-58(n, γ)Fe-59 reaction. The two thermal curves are in general agreement with one another. The calculated values are somewhat high at the core end of the curve and low

[redacted]

at the edge end relative to the experimental values. The agreement between the experimental data and the calculated values in the low flux region is actually better than shown since some of the neutrons in what is defined here as the epithermal region, contribute to the Fe-58(n, γ) Fe-59 reaction. This contribution will enhance the "thermal" flux, particularly at the lower end of the range. It will not be sufficient, however, to give the reflection caused enhancement equal to that seen in the experimental data.

Flux Enhancement Test Section (FETS)

No flux monitors were placed in the FETS. However, based on the TS4U and TS4D thermal flux data and an interpolation to the FETS, it is estimated that the thermal flux was about 3.7×10^{13} n/cm^{2}sec (based on a core value of 3.9×10^{13} n/cm^{2}sec which is based on a Run 4 operating power level - Run 6 was actually 7.5% lower than this).

According to calculations performed by the BNW Analytical Physics Section, the β flux at the center of the surface of the test specimen is about 3.6×10^{11} β/cm^{2}sec (which is equivalent to 57 nano-amperes/cm^2) (based on 3.9×10^{13} n/cm^{2}sec). On the centerline of the specimen, but well away from the rhodium, the β flux due to the Zircaloy is approximately 2.7×10^7 β/cm^{2}sec (4 picoamperes/cm^2). Thus the rhodium provides a 13,000 fold enhancement of the β flux, at the test specimen surface. Figure 5 shows the calculated β flux profile across the specimen as well as along its axis at both the surface of the test specimen and at the top of the water channel.

Within 0.050 - 0.100 inch of the edge of the rhodium, in a horizontal direction, the beta flux reaches a steady state value. Thus the flux is essentially constant on the test specimen. The beta flux at the specimen

DECLASSIFIED

FIGURE 5 - Beta Flux Profile in FETS.

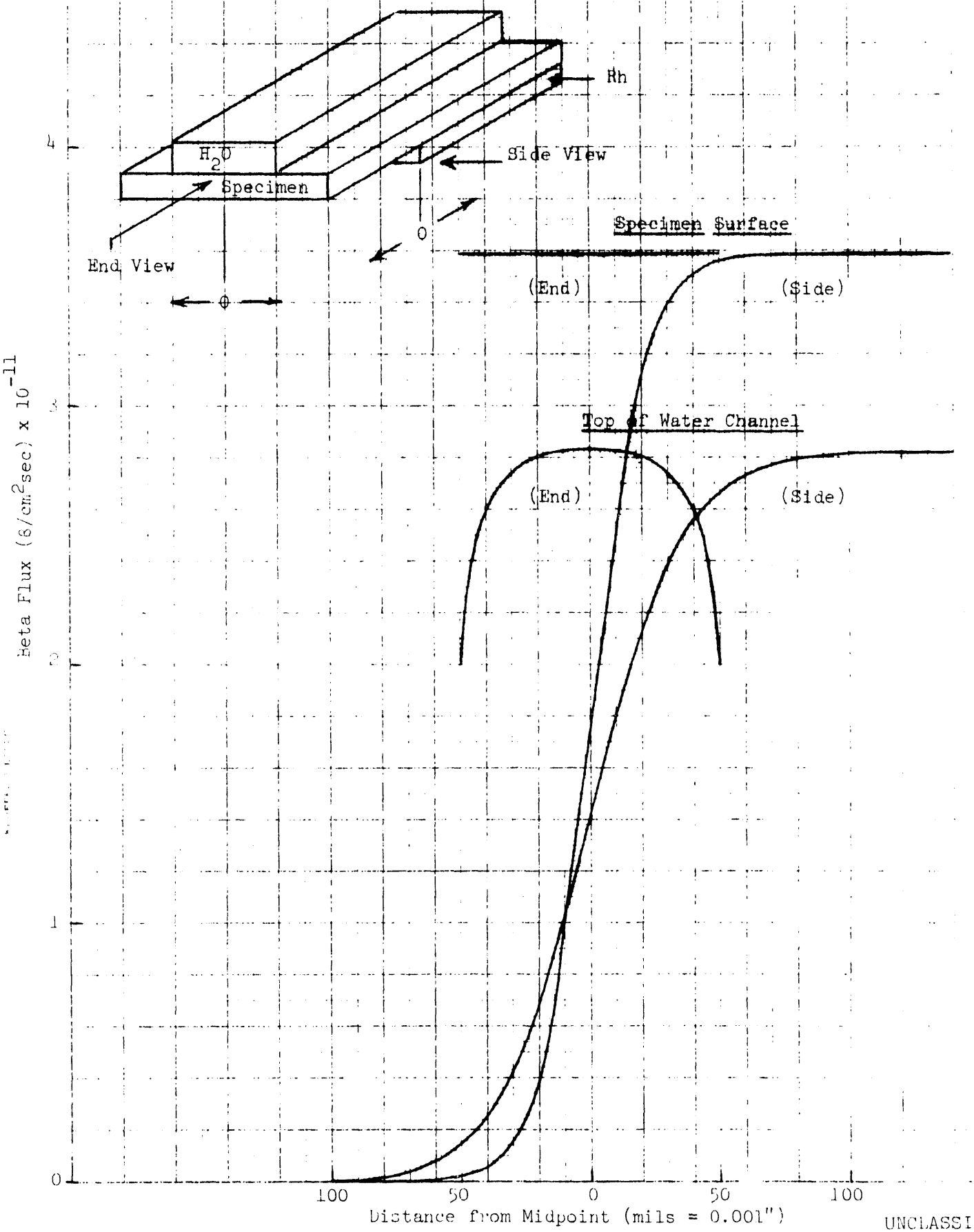

surface is about 22% greater than at the centerline at the top of the water channel. It is about 44% greater than that at the edges of the top of the water channel. On the average the beta flux drops 30% in passing through the 0.025 inch thick water channel.

Thus 0.30 (57 n-amp/cm^2) = 17.1 n-amp/cm^2 is absorbed by the water and must find its way back to the metal electrochemically. About one-half of this could be returned to the metal via the specimen surface and could effect chemical changes on the surface.

In addition to the enhanced beta flux, the gamma flux will increase. According to Mittelman and Liedtke* each capture of a thermal neutron by zirconium results in a release of about 6 MeV of gamma energy. Similarly rhodium emits about 4 MeV per capture. Furthermore, the rhodium is about 4.6×10^4 stronger a source than an equivalent amount of zirconium. The exact amount of enhancement can not be determined at this time however. This calculation will be performed after the neutron spectra is determined and it is possible to calculate the effect of the surrounding material.

*Mittelman, P.S. and R.A. Liedtke, Gamma Rays from Thermal Neutron Capture, Nucleonics 13 (5) 50-51 (1955).

DATE FILMED

9/29/94

END